PERGAMON

International Journal of Mechanical Sciences 43 (2001) 455–470

International Journal of MECHANICAL SCIENCES

www.elsevier.com/locate/ijmecsci

Decay rate of edge effects in cross-ply-laminated hollow cylinders

Jianqiao Ye*

Department of Civil Engineering, The University of Leeds, Leeds, LS2 9JT, UK

Received 17 August 1998; received in revised form 15 December 1999; accepted 12 January 2000

Abstract

The decay rates of stresses and displacements due to self-equilibrated loads acting on the end of cross-ply-laminated hollow cylinders are found by using the theory of three-dimensional elasticity. The study assumes that the periodic displacement and stresses fields used decay away exponentially from the end load region. The use of a recursive and successive approximation method leads to an eigenmatrix whose eigenvalues represent the decay rates of the problem. By this approach, the composite cylinders may be composed of an arbitrary number of orthotropic layers, each of which may have different material properties and thicknesses. The eigenvalue problem has always a dimension of 3×3, regardless of the number of the layers. The decay rates for either symmetric or antisymmetric cross-ply-laminated cylinders are found and presented. The effects of material properties on decay rates are investigated for a typical eight-layered anti-symmetric cross-ply-laminated cylinder. The displacement and stress distributions across thickness of cylinders for selected problems are also presented. © 2000 Elsevier Science Ltd. All rights reserved.

Keywords: Decay rate; Composites; Three-dimensional elasticity; Edge-effect

1. Introduction

The edge effects of hollow cylinders subjected to self-equilibrated end loads have been the subject of extensive investigations and the history of the analysis has been well documented in the literature (see e.g. Refs. [1,2]). The majority of the worked reported in the area were based on Toupin [3] and Knowle's [4] theorem that provides upper bound estimates of the strain energy (E)

* Fax: + 44-0113-2332265.
E-mail address: j.ye@leeds.ac.uk (J. Ye).

PII: S0020-7403(00)00011-4

Nomenclature

a	inner radius of cylinder
b	out radius of cylinder
C_{ij}	elastic constants of materials
E	strain energy of elastic body
E_L, E_T	elastic modulus in axial, or transverse direction
G_{LT}, G_{TT}	shear modulus
$h, h^{(j)}$	thickness of cylinder or the jth sub-cylinder
k	decay rate (characteristic decay length)
n	circumferential wave number
r, R	radius or mean radius of hollow cylinder
$R^{(j)}$	mean radius of the jth sub-cylinder or sub-layer
u, v, w	axial, circumferential, and radial displacements
x, s, z	axial, circumferential, and radial co-ordinates
ε_{ii}	direct strain component ($i = x, s, z$)
γ_{ij}	shear strain component ($i, j = x, s, z$)
λ_i	eigenvalue of $\mathbf{G}$
σ_{ii}	direct stress component ($i = x, s, z$)
τ_{ij}	shear stress component ($i, j = x, s, z$)
ν_{LT}, ν_{TT}	Poisson's ratio

in a body as a function of the distance (z) away from the region of applied tractions, i.e.,

$$E(z) \leqslant E(0)\exp(-kz), \tag{1}$$

where k is the inverse of the characteristic decay length that represents the decay rate of strain energy towards the interior zone of the body, $E(0)$ is the total strain energy, and $E(z)$ is the strain energy in the part of the body beyond z. Because of the quadratic nature of strain energy in terms of the mechanical variables, the estimates of displacements and stresses in the body can be subsequently factored as follows:

$$\begin{aligned} &(u, v, w) \leqslant K_1 \exp(-kz), \\ &\sigma_{ij} \leqslant K_2 \exp(-kz), \end{aligned} \quad (i, j = x, s, z), \tag{2}$$

where K_1 and K_2 are constants. On the basis of above theorem, most published work assumed that any self-equilibrated edge stress decay away exponentially from the loaded end. For structures made of isotropic linear elastic materials, extensive work has been done either analytically (see e.g. Ref. [5]) or numerically (see e.g. Refs. [6,7]). For elastic hollow cylinders, Stephen and Wang [8] presented an analytical solution by which exact decay rates can be found in the context of three-dimensional consideration.

It has been recognised that composite materials are considerably more sensitive in edge effects than isotropic materials. Experimental results [9] have shown that edge effects may persist much farther into composite materials than for isotropic ones. As a result of this, the edge effects in composites cannot be simply neglected and also the experience gained in isotropic cases may not be applied directly to anisotropic materials. Moreover, high-level transverse normal and shear stresses acting in the region near the free edge of laminated composites are the major concern on the material failure due to delamination. Hence, it is vitally important for composite manufacturers and users to have a better understanding of the edge effects on such materials. This may help them to tailor a material with specific properties so that edge stresses can decay at a desired rate. As laminated composite materials have been increasingly used by various industries, considerable attention in this respect has been received in the last two decades. Both numerical and analytical approaches have been used to determine decay rates in composite materials. For instance, Finite element method was used to find the decay rates of laminated plates [10]. Although this method is probably one of the most universal methods which can be applied to problems involving any cross-section, it is sometimes quite computationally expensive, especially for multi-layered laminates. For laminates having regular cross-sections, analytic method is still a powerful tool to be used for the purpose. However, due to the complex nature of anisotropy, many recently published results were confined to examine edge effects on laminated materials having simple displacement and stress fields [11–13].

On the basis of three-dimensional elasticity consideration, this paper studies the decay rates of cross-ply-laminated hollow cylinders subjected to self-equilibrated end loads. The analytic technique presented herein is based on the recursive and successive approximation method which has been successfully used in connection with buckling and vibration analysis of cross-ply-laminated cylinders [14,15]. Previous numerical experience has shown that buckling and vibration results obtained from this method converge very fast to the corresponding three-dimensional solutions. In this paper, this method is modified and used to deal with edge-effect problems by solving an (3×3) eigensystem whose general eigenvalues (including complexes) give the decay rates of the problem. The order of the final eigensystem is independent of the number of the orthotropic layers of a laminate. Hence this method is particularly useful for either thick or thin laminates having a large number of layers.

Parametric investigations are presented in the paper for eight-layered symmetric and antisymmetric cylinders having various thickness ratios. The decay rates of these cylinders are shown for selected circumferential modes. The effect of material anisotropy on the lowest decay rate of a eight-layered antisymmetric cylinder is shown in graphic form. For selected decay modes, the corresponding stress and displacement patterns are also presented to show a general picture of their distribution near the end of the laminates.

2. Formulation of a exponential decay problem

Consider a hollow circular cylinder (Fig. 1) having a constant thickness h and middle-surface radius R. The axial, circumferential and normal to the middle-surface co-ordinates are denoted by x, s and z, respectively, while u, v and w represent the corresponding displacements. It is assumed that the cylinder is made of a homogeneous, orthotropic, linearly elastic material. Accordingly, its

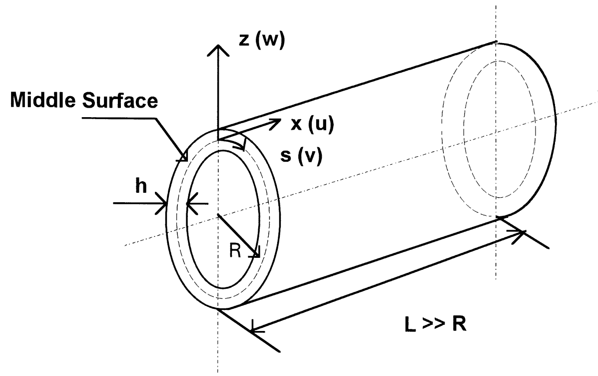

Fig. 1. Nomenclature of a hollow cylinder.

elastic behaviour is described by the Hook's law

$$\begin{Bmatrix} \sigma_x \\ \sigma_s \\ \sigma_z \\ \tau_{sz} \\ \tau_{xz} \\ \tau_{xs} \end{Bmatrix} = \begin{bmatrix} C_{11} & C_{12} & C_{13} & 0 & 0 & 0 \\ C_{12} & C_{22} & C_{23} & 0 & 0 & 0 \\ C_{13} & C_{23} & C_{33} & 0 & 0 & 0 \\ 0 & 0 & 0 & C_{44} & 0 & 0 \\ 0 & 0 & 0 & 0 & C_{55} & 0 \\ 0 & 0 & 0 & 0 & 0 & C_{66} \end{bmatrix} \begin{Bmatrix} \varepsilon_{xx} \\ \varepsilon_{ss} \\ \varepsilon_{zz} \\ \gamma_{sz} \\ \gamma_{xz} \\ \gamma_{xs} \end{Bmatrix}. \tag{3}$$

In cylindrical co-ordinates the three-dimensional differential equations of equilibrium and the strain–displacement relations are, respectively, as follows:

$$\frac{\partial \sigma_{xx}}{\partial x} + \frac{\partial \tau_{xs}}{\partial s} + \frac{\partial \tau_{xz}}{\partial z} + \frac{\tau_{xz}}{r} = 0,$$

$$\frac{\partial \tau_{xs}}{\partial x} + \frac{\partial \sigma_{ss}}{\partial s} + \frac{\partial \tau_{sz}}{\partial z} + \frac{2\tau_{sz}}{r} = 0,$$

$$\frac{\partial \tau_{xz}}{\partial x} + \frac{\partial \tau_{sz}}{\partial s} + \frac{\partial \sigma_{zz}}{\partial z} + \frac{\sigma_{zz} - \sigma_{ss}}{r} = 0, \tag{4}$$

$$\begin{aligned} &\varepsilon_{xx} = \frac{\partial u}{\partial x}, \quad \varepsilon_{ss} = \frac{\partial v}{\partial s} + \frac{w}{r}, \quad \varepsilon_{zz} = \frac{\partial w}{\partial z}, \\ &\varepsilon_{xs} = \frac{\partial v}{\partial x} + \frac{\partial u}{\partial s}, \quad \varepsilon_{xz} = \frac{\partial w}{\partial x} + \frac{\partial u}{\partial z}, \quad \varepsilon_{sz} = \frac{\partial w}{\partial s} + \frac{\partial v}{\partial z} - \frac{v}{r}, \end{aligned} \tag{5}$$

where $r = R + z$. After eliminating the three membrane stresses from Eqs. (3)–(5), the governing equation of a three-dimensional elasticity problem in cylindrical co-ordinates can be represented as a set of linear differential equations with respect to z:

$$
\begin{aligned}
&\frac{\partial u}{\partial z} = -\frac{\partial w}{\partial x} + \frac{\tau_{xz}}{C_{55}},\\
&\frac{\partial v}{\partial z} = \frac{v}{r} - \frac{\partial w}{r\partial \theta} + \frac{\tau_{sz}}{C_{44}},\\
&\frac{\partial w}{\partial z} = C_1\frac{\partial u}{\partial x} - C_5\frac{\partial v}{r\partial \theta} - C_5\frac{w}{r} + C_6\sigma_{zz},\\
&\frac{\partial \sigma_{zz}}{\partial z} = C_3\frac{\partial u}{r\partial x} + C_4\frac{\partial v}{r^2\partial \theta} + \frac{C_4 w}{r^2} - \frac{(1+C_5)}{r}\sigma_{zz} - \frac{\partial \tau_{sz}}{r\partial \theta} - \frac{\partial \tau_{xz}}{\partial x},\\
&\frac{\partial \tau_{xz}}{\partial z} = \left(-C_2\frac{\partial^2}{\partial x^2} - C_{66}\frac{\partial^2}{r^2\partial \theta^2}\right)u - (C_3 + C_{66})\frac{\partial^2 v}{r\partial x\partial \theta} - C_3\frac{\partial w}{r\partial x} + C_1\frac{\partial \sigma_{zz}}{\partial x} - \frac{\tau_{xz}}{r},\\
&\frac{\partial \tau_{sz}}{\partial z} = -(C_3 + C_{66})\frac{\partial^2 v}{r\partial x\partial \theta} + \left(-C_{66}\frac{\partial^2}{\partial x^2} - C_4\frac{\partial^2}{r^2\partial \theta^2}\right)v - C_4\frac{\partial w}{r\partial \theta} + C_5\frac{\partial \sigma_{zz}}{r\partial \theta} - \frac{2\tau_{sz}}{r}.
\end{aligned}
\tag{6}
$$

In Eq. (6) the constants C_i $(i = 1, 2, \ldots, 5)$ are as follows:

$$
\begin{aligned}
&C_1 = -C_{13}/C_{33}, \quad C_2 = C_{11} - C_{13}^2/C_{33}, \quad C_3 = C_{12} - C_{13}C_{23}/C_{33},\\
&C_5 = -C_{23}/C_{33}, \quad C_4 = C_{22} - C_{23}^2/C_{33}, \quad C_6 = 1/C_{33}.
\end{aligned}
\tag{7}
$$

According to the theorems of Toupin and Knowles [3] and the estimated displacements and stresses of (2), for the decay problem of a cylinder, the following exponential decay and periodic displacements and the associated transverse stress fields can be used:

$$
\begin{aligned}
u &= U(z)e^{in\theta}e^{-kx},\\
v &= V(z)e^{in\theta}e^{-kx},\\
w &= W(z)e^{in\theta}e^{-kx},
\end{aligned}
\tag{8}
$$

$$
\begin{aligned}
\sigma_{zz} &= Z(z)e^{in\theta}e^{-kx},\\
\tau_{xz} &= X(z)e^{in\theta}e^{-kx},\\
\tau_{sz} &= S(z)e^{in\theta}e^{-kx},
\end{aligned}
\tag{9}
$$

where n is the circumferential wave number and $\mathrm{i} = \sqrt{-1}$, k is the decay rate of edge stresses and displacements of the cylinder. Substitution of Eqs. (8) and (9) into Eq. (6) gives the following matrix form of a first-order differential equation system in terms of displacements and three transverse stresses:

$$
\frac{\partial}{\partial z}\{\mathbf{F}\} = [\mathbf{G}]\{\mathbf{F}\}, \quad \{\mathbf{F}\} = [W(z)\ U(z)\ iV(z)\ Z(z)\ X(z)\ iS(z)]^{\mathrm{T}},
\tag{10}
$$

where i is used to indicate the $\pi/2$ phase difference between v and its counterparts u and w and also between transverse stress τ_{sz} and two other transverse stresses σ_{zz} and τ_{xz}. The 6×6 matrix $[\mathbf{G}]$ in Eq. (10) has the following form:

$$[\mathbf{G}] = \begin{bmatrix} \dfrac{C_5}{R} & -C_1 k & \dfrac{nC_5}{R} & C_6 & 0 & 0 \\ k & 0 & 0 & 0 & \dfrac{1}{C_{55}} & 0 \\ \dfrac{n}{R} & 0 & \dfrac{1}{R} & 0 & 0 & \dfrac{1}{C_{44}} \\ \dfrac{C_4}{R^2} & -\dfrac{C_3 k}{R} & \dfrac{nC_4}{R^2} & -\dfrac{(1+C_5)}{R} & k & -\dfrac{n}{R} \\ \dfrac{C_3 n}{R^2} & -C_2 k^2 + \dfrac{n^2 C_{66}}{R^2} & \dfrac{nk(C_3+C_{66})}{R} & -C_1 k & \dfrac{-1}{R} & 0 \\ \dfrac{C_4 n}{R^2} & -\dfrac{nk(C_3+C_{66})}{R} & -C_{66}k^2 + \dfrac{n^2 C_4}{R^2} & -\dfrac{nC_5}{R} & 0 & -\dfrac{2}{R} \end{bmatrix}.$$

It is noticed that the term $1/R$ has been used in the matrix to replace the term $1/r$, where $r = R(1 + z/R)$. For cylinders having small thickness ($h/R \ll 1$), such a replacement is reasonable [14]. As a result, matrix $[\mathbf{G}]$ is a constant complex matrix in general since k can be a complex.

To find the decay rates, the cylinder is assumed to be free of external tractions on the surface generators and, therefore, the following stress boundary conditions are imposed on the lateral cylindrical surfaces $z = \pm h/2$:

$$\sigma_{zz}(\pm h/2) = 0, \quad \sigma_{sz}(\pm h/2) = 0 \quad \text{and} \quad \sigma_{xz}(\pm h/2) = 0. \tag{11}$$

The general solution of Eq. (10) can be explicitly expressed as

$$\{\mathbf{F}(z)\} = [\mathbf{B}(z)]\{\mathbf{F}(-h/2)\} \quad (-h/2 \leqslant z \leqslant h/2). \tag{12}$$

In Eq. (12) $[\mathbf{B}(z)] = [\mathbf{Q}]^{-1} diag[\mathrm{e}^{\lambda_1 (z+h/2)}\mathrm{e}^{\lambda_2 (z+h/2)} \ldots \mathrm{e}^{\lambda_n (z+h/2)}][\mathbf{Q}]$ where the λ_i ($i = 1,2,\ldots,6$) are the distinctive eigenvalues of $[\mathbf{G}]$ and are in general complex. $[\mathbf{Q}]$ is a (6×6) matrix consisting of six independent eigenvectors corresponding to the eigenvalues. In the cases of repeated eigenvalues of $[\mathbf{G}]$, existing methods, e.g. Cayley–Hamilton method [16], can be used to evaluate $[\mathbf{B}(z)]$ analytically (see the appendix). However, numerical experience showed that for cylindrical layers the eigenvalues of $[\mathbf{G}]$ are likely to be distinctive while repeated eigenvalues occur only when isotropic flat layers are considered.

When $z = h/2$, Eq. (12) becomes

$$\{\mathbf{F}(h/2)\} = [\mathbf{B}(h/2)]\{\mathbf{F}(-h/2)\} \tag{13.1}$$

or

$$\begin{Bmatrix} W(h/2) \\ U(h/2) \\ iV(h/2) \\ 0 \\ 0 \\ 0 \end{Bmatrix} = \begin{bmatrix} B_{11} & B_{12} & B_{13} & B_{13} & B_{14} & B_{15} \\ B_{21} & B_{22} & B_{23} & B_{24} & B_{25} & B_{26} \\ B_{31} & B_{32} & B_{33} & B_{34} & B_{35} & B_{36} \\ B_{41} & B_{42} & B_{43} & B_{44} & B_{45} & B_{46} \\ B_{51} & B_{52} & B_{53} & B_{54} & B_{55} & B_{56} \\ B_{61} & B_{62} & B_{63} & B_{64} & B_{65} & B_{66} \end{bmatrix} \begin{Bmatrix} W(-h/2) \\ U(-h/2) \\ iV(-h/2) \\ 0 \\ 0 \\ 0 \end{Bmatrix} \tag{13.2}$$

after introducing boundary conditions (11). Here $\{\mathbf{F}(-h/2)\}$ and $\{\mathbf{F}(h/2)\}$ denote the values of the vector $\{\mathbf{F}\}$ at the bottom ($z = -h/2$) and top ($z = h/2$) surfaces of the cylinder, respectively. In Eq. (13.2), the B_{ij} are in general functions of the decay rate k.

The bottom half of above equation gives

$$\begin{bmatrix} B_{41} & B_{42} & B_{43} \\ B_{51} & B_{52} & B_{53} \\ B_{61} & B_{62} & B_{63} \end{bmatrix} \begin{Bmatrix} W(-h/2) \\ U(-h/2) \\ iV(-h/2) \end{Bmatrix} = \begin{Bmatrix} 0 \\ 0 \\ 0 \end{Bmatrix}. \tag{14}$$

To ensure that there is a non-zero displacement field at the edge of the cylinder, the decay rate k must be of the values at which the following 3×3 complex determinant is nullified:

$$\det \begin{bmatrix} B_{41} & B_{42} & B_{43} \\ B_{51} & B_{52} & B_{53} \\ B_{61} & B_{62} & B_{63} \end{bmatrix} = 0. \tag{15}$$

Hence the zeros of above equation give the decay rates of the composite cylinder subjected to self-equilibrated end forces. For a thin cylinder the above calculations can provide decay rates which are very close to the corresponding three-dimensional ones. As a matter of fact, the calculated decay rates approaches to the three-dimensional solutions as h/R approaches zero.

To calculate the decay rates of a thick or laminated cylinder, the solution of Eq. (10) is based on the division of the hollow cylinder into N coaxial and successive fictitious sub-cylinders. Different layers may have different thicknesses and material properties. However, it is assumed that the thickness of each layer approaches zero uniformly as N approaches infinity. Assuming, in addition, that each sub-layer is homogeneous and made of an orthotropic elastic material, two types of material interfaces are distinguished in such a cross-ply laminate: the fictitious interfaces that separate layers with same material properties and the real ones that separate layers of different materials. For each of these sub-cylinders the approximate solution (12) or (13.1) is initially formed. Upon choosing a suitably large value of N, each individual layer becomes thin, i.e., $h^{(j)}/R^{(j)} \ll 1$, where $h^{(j)}$ and $R^{(j)}$ are, respectively, the thickness and middle surface radius of the jth sublayer. As a result, an approximate solution of the form described in the preceding sections is considered adequate. All solutions obtained are then connected through imposing continuity conditions on the fictitious and real interfaces to form a solution that provide with an approximate decay rates of the thick or/and laminated cylinder which again are very close to the corresponding three-dimensional solutions as long as N is sufficiently large.

Dealing in particular with the interface of the $(j-1)$th and jth of the afore-mentioned fictitious layers, having thicknesses $h^{(j-1)}$ and $h^{(j)}$, respectively, the continunity of displacements and transverse stresses at the interfaces leads to following relation $(j = 2, \dots, N)$:

$$\{\mathbf{F}^{(j)}(-h^{(j)}/2)\} = \{\mathbf{F}^{(j-1)}(h^{(j-1)}/2)\}. \tag{16}$$

Hence, upon recursively using Eqs. (13.1) and (16), the following equation can be found for the N-layered composite cylinder:

$$\begin{aligned}\{\mathbf{F}^{(N)}(h^{(N)}/2)\} &= [\mathbf{B}^{(N)}(h^{(N)}/2)]\{\mathbf{F}^{(N)}(-h^{(N)}/2)\}\\ &= [\mathbf{B}^{(N)}(h^{(N)}/2)]([\mathbf{B}^{(N-1)}(h^{(N-1)}/2)]\{\mathbf{F}^{(N-1)}(h^{(N-1)}/2)\})\\ &= [\mathbf{H}^{[N]}]\{\mathbf{F}^{(1)}(-h^{(1)}/2)\},\end{aligned} \tag{17}$$

where

$$[\mathbf{H}^{(N)}] = \prod_{i=N}^{1} [\mathbf{B}^{(i)}(h^{(i)}/2)] \tag{18}$$

which is an equivalent matrix to $[\mathbf{B}]$ in Eq. (13.1). By considering boundary conditions (11), Eq. (17) also yields an eigenvalue problem, the solutions of which are the decay rates of the laminated cylinder. It is worth mentioning that, since $[\mathbf{H}]$ has the same dimension as that of $[\mathbf{B}]$, the decay rates can still be found as the roots of a 3×3 eigen-determinant, independently of the number of real and/or fictitious layers involved. After the eigenvalues have been found, the associated eigenvectors, i.e., the displacement modes at $z = -h/2$, can be found from Eq. (17). The modes showing displacement and transverse stress ditributions across the thickness can then be obtained below by following Eq. (12):

$$\{\mathbf{F}^{(k)}(z)\} = [\mathbf{H}^{(k)}(z)]\{\mathbf{F}^{(1)}(-h^{(1)}/2)\} \quad (k = 1, 2, \dots, N, -h^{(k)}/2 \leqslant z \leqslant h^{(k)}/2), \tag{19}$$

where

$$[\mathbf{H}^{(k)}] = [\mathbf{B}^{(k)}(z)] \prod_{i=k-1}^{1} [\mathbf{B}^{(i)}(h^{(i)}/2)]. \tag{20}$$

3. Numerical results and discussion

As has been shown in previous publications dealing with stability and dynamic analyses of cross-ply-laminated cylinders [14,15] numerical results obtained on the basis of the recursive and successive approximation approach converge very rapidly to the corresponding results based on alternative three-dimensional solutions. Using relatively thin sub-cylinders ($h^{(j)}/R^{(j)} < 0.02$, $j = 1, 2, \dots, N$) in such comparisons, it was found that the results obtained normally had an accuracy at least up to four significant figures. Following this observation, the number of fictitious layers employed for the derivation of all of the results shown in this section was chosen such that $h^{(j)}/R^{(j)} < 0.02$ is always satisfied. Dealing with complex eigenvalues and related problems of complex matrices, NAG library was used in the calculations.

In this section, the decay rates of an eight-layered cross-ply-laminated cylinder with either symmetric or antisymmetric lay-ups are presented through a parametric study. For the purpose of comparisons, the decay rates were calculated first for isotropic cylinders for which exact three-dimensional solutions are available in the literature [8]. The results presented in Table 1 are the non-dimensional decay rate parameter (kb) of an isotropic cylinder having $a/b = 0.5$ or 0.8, where a and b are the inner and outer radius of the cylinder, respectively. The first four decay rate parameters for the first three circumferential modes ($n = 0, 1, 2$) are given in the table, in which the real values are associated with exponential decay while the complex ones are corresponding to damped sinusoidal decay. The results in Table 1 have been compared with the graphic solution presented by Stephen and Wang [8] and a good agreement has been observed.

After the successful comparisons, the method was then used to find the decay rates of an eight-layered cross-ply-laminated cylinder with either symmetric or antisymmetric lay-ups. Each material layer has the same thickness. The results were obtained for a thick cylinder ($a/b = 0.5$) and a moderately thick one with $a/b = 0.8$. Three circumferential modes were considered, i.e., $n = 0$, 1 and 2 and the first five decay rate parameters were calculated for each case. In the calculations, the following fibre reinforced material properties were used:

$$E_L/E_T = 10, \quad G_{LT}/E_T = 0.6, \quad G_{TT}/E_T = 0.5, \quad v_{LT} = v_{TT} = 0.25, \tag{21}$$

where subscripts L and T indicate longitudinal and transverse directions of the fibres.

Tables 2 and 3, respectively, show the decay rate parameter of the eight-layered antisymmetrically laminated cylinder with $a/b = 0.5$ and 0.8, while Tables 4 and 5 give the parameters for the corresponding symmetrically laminated ones.

For antisymmetric cylinders, the results presented in Tables 2 and 3 show that for thicker cylinder ($a/b = 0.5$) the lowest decay rate parameters (lowest real or real part of a complex) for the three cases ($n = 0, 1, 2$) are always real while for thinner cylinder ($a/b = 0.8$) they are all complexes. For lower circumferential wave numbers ($n = 0, 1$) the lowest decay rate parameter increases as the thickness decreases. For higher circumferential modes ($n = 2$), however, the lowest decay rate parameter decreases as the thickness decreases. This is coincident with the observation made for isotropic cases [8]. Similar conclusions can also be made for symmetric cases (see Tables 4 and 5).

Table 1
Decay rates (kb) of an isotropic cylinder

	$n = 0$	$n = 1$	$n = 2$
	$2.4058 \pm i1.9082$	$2.7741 \pm i1.4421$	$1.3341 \pm i0.7477$
$a/b = 0.5$	6.8139	7.0142	$3.9995 \pm i0.8189$
	$8.6072 \pm i4.4975$	$8.6918 \pm i4.4295$	7.5933
	12.8556	12.9432	$8.9410 \pm i4.2312$
	$3.1737 \pm i2.9448$	$3.3692 \pm i2.7357$	$0.7510 \pm i0.5364$
$a/b = 0.8$	15.8554	15.8964	$4.0299 \pm i2.2909$
	$21.1071 \pm i11.2539$	$21.1301 \pm i11.2411$	16.0189
	31.4903	31.5104	$21.1989 \pm i11.2029$

Table 2
Decay rate parameter (kb) for antisymmetrically laminated cylinder ($a/b = 0.5$, $[0/90]_4$)

$n = 0$	$n = 1$	$n = 2$
2.2785	1.7111	1.0709
4.3313 ± i0.0883	4.2857	1.5076 ± i0.5593
5.4222	5.4635 ± i0.1742	4.3917
6.4963	8.2472	5.7226
10.5848 ± i3.0212	10.6967 ± i2.7489	7.4216

Table 3
Decay rate parameter (kb) for antisymmetrically laminated cylinder ($a/b = 0.8$, $[0/90]_4$)

$n = 0$	$n = 1$	$n = 2$
3.6986 ± i2.4196	4.0710 ± i1.7154	0.8205 ± i0.3429
10.7459	1.7525	2.8725
14.0695	14.0876	7.2847
15.1166	15.4896	10.7642
25.1971 ± i2.4196	25.2295 ± i6.9419	14.1125

Table 4
Decay rate parameter (kb) for symmetrically laminated cylinder ($a/b = 0.5$, $[0/90/0/90]_s$)

$n = 0$	$n = 1$	$n = 2$
1.9929	1.5610	1.1257
4.4216 ± i0.5608	4.4503	1.3447 ± i0.4216
4.6135	5.0483 ± i0.4194	4.5664
6.5754	7.7061	5.1037
11.0456 ± i1.6251	11.5679 ± i1.2826	6.7911

Table 5
Decay rate parameter (kb) for symmetrically laminated cylinder ($a/b = 0.8$, $[0/90/0/90]_s$)

$n = 0$	$n = 1$	$n = 2$
3.4805 ± i2.2028	3.8608 ± i1.4247	0.7340 ± i0.3582
10.2833	11.2942	2.5564
12.4326	12.4399	7.2444
15.3002	15.5989	11.3209
24.0842	24.1785	12.4524

Fig. 2 shows the minimum decay rate parameters for the first three circumferential modes of an eight-layered antisymmetric cylinder with $a/b = 0.8$. The material properties described in Eq. (20) are used for the cylinder except that the ratio between E_L and E_T is now allowed to vary. The decay rate parameters are calculated and plotted against the ratio. For complex decay rates, only real parts of them are plotted and shown by dotted lines. The solid lines in the figure represent real decay rates.

It is clear from Fig. 2 that the decay rates for all the cases are in general decreasing as the cylinder becomes more anisotropic although some increases of them have been observed when the ratio, E_L/E_T is small. It is also clear from the figure that for small values of E_L/E_T, damped sinusoidal modes dominate the decay while for higher values of E_L/E_T, the lowest decay modes are always associated with exponential decay. These observations can also be found from Fig. 3 which shows the lowest decay rate parameters of a laminated cylinder with various section profiles. In Fig. 3 the decay rate parameter associated with $n = 1$ are presented for cylinders having 0°, 90°, and

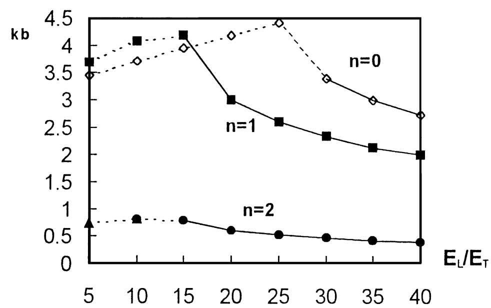

Fig. 2. Decay rate parameter of an eight-layered antisymmetrically laminated cylinder.

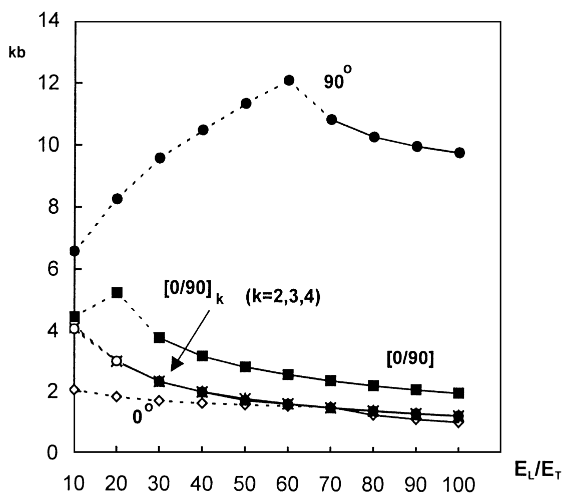

Fig. 3. Decay rate parameter of antisymmetrically laminated cylinders against layer numbers.

$[0°/90°]_k$ ($k = 1, 2, 3, 4$) profile, respectively. Comparing the decay rate parameters of these cylinders, it can be seen that the 0° cylinder always gives lowest rates while the 90° cylinder always gives the highest ones, which can be used as upper or lower bound estimate in design. The decay rates for cylinders having more than four antisymmetric layers are essentially the same and decrease as the ratio, E_L/E_T, increases. For the 90° and 0°/90° cylinders, the decay rates decrease following some increases when the materials are less anisotropic. Comparing with corresponding isotropic case (see Table 1), except the 90° cylinder, the decay rate parameters of the laminated cylinders become about three times smaller than those of corresponding isotropic case when E_L/E_T approaches 100. Hence, it is evident that for laminated materials, especially highly anisotropic materials the edge effects are significant and the characteristic decay length may be several times longer than the corresponding length for isotropic cases.

To find stress and displacement distributions across the thickness of a composite cylinder, the applied self-equilibrium end stress has to be represented as an complete eigenvector expansion associated with the complete set of eigenvalues, i.e., the decay rates, obtained. This will involve orthogonalisation of eigenvectors and treatment of singularities for concentrated loads. Future research is needed in the respect. To illustrate stress and displacement field associated with given

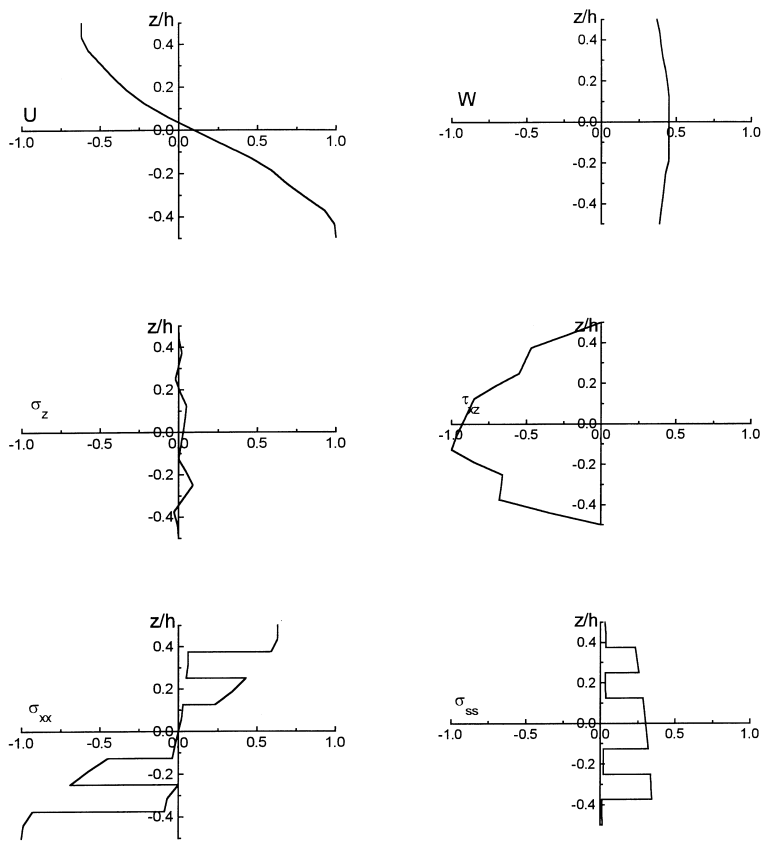

Fig. 4. Displacement and stress distributions for $n = 0$.

decay rates, the relative displacement and stress distributions across the thickness for selected modes are found and presented in Figs. 4–6 for the eight-layered symmetric cylinder having $a/b = 0.5$. The displacements, transverse and membrane stresses are scaled separately so that the maximum values of each of them are unit. Three cases are considered. They are for the three lowest decay parameters, i.e., $kb = 1.9929$, 1.5610 and 1.1257, corresponding to, respectively, decay modes $n = 0$, 1 and 2.

In Fig. 4, the results for $n = 0$ are presented where there are no circumferential displacement, shear stresses τ_{xs} and τ_{sz}. Obviously, these are associated with a torsionless axisymmetric mode. From Fig. 4, it is observed that the displacement u, transverse shear stress τ_{xz} and membrane stress σ_{xx} are more significant than their counterparts. It can also be observed that the decay mode is associated with the end loading characterised by distributed bending moments about the mid-line of the section and shear forces in radial direction (see the distribution of σ_{ss} and τ_{sz} and τ_{xs}).

In Fig. 5, the results for $n = 1$ are presented. Once again, the displacement u, transverse shear stress τ_{xz} and membrane stress σ_{xx} are predominant. There are also quite significant circumferential and transverse displacements across the thickness. The mode is associated with the end loading characterised by distributed bending moments about the mid-line of the section, shear forces in radial direction and applied torques on the section (see the distribution of σ_{xx} and τ_{xz} and τ_{xs}).

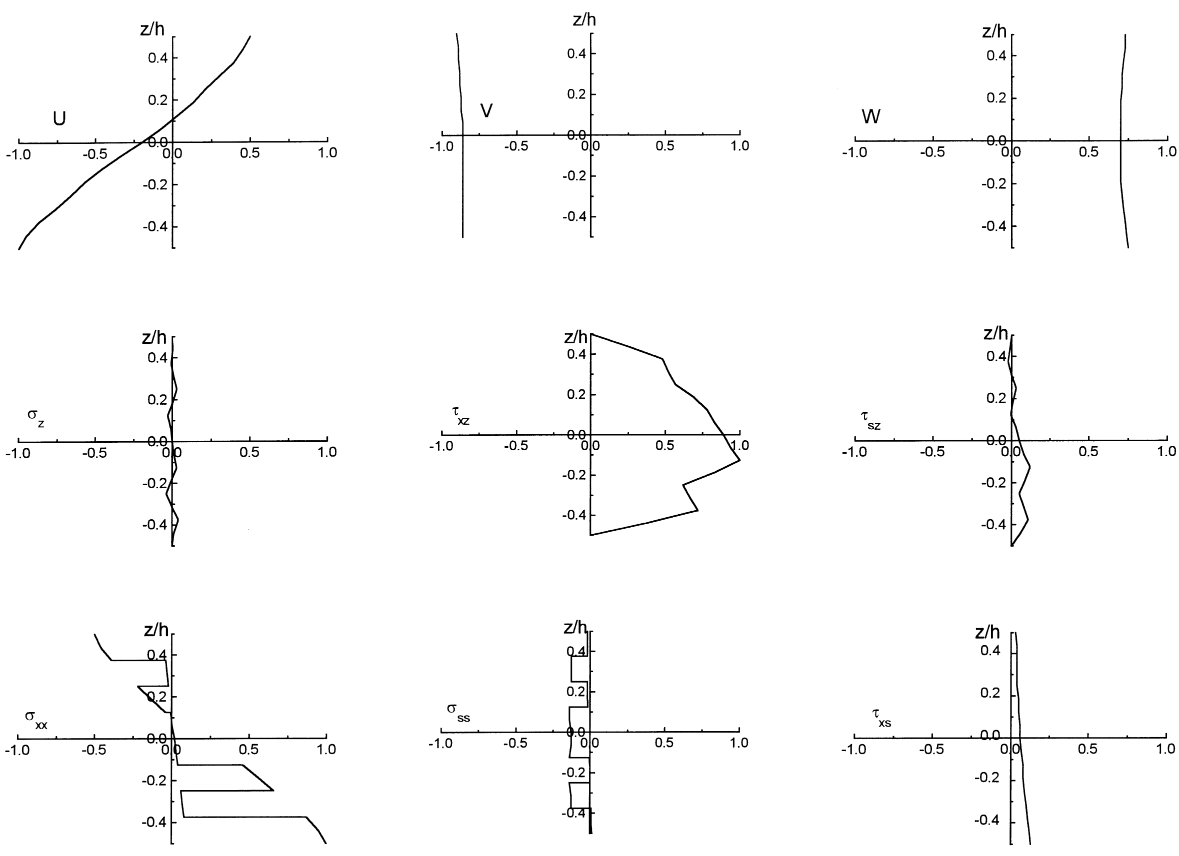

Fig. 5. Displacement and stress distributions $n = 1$.

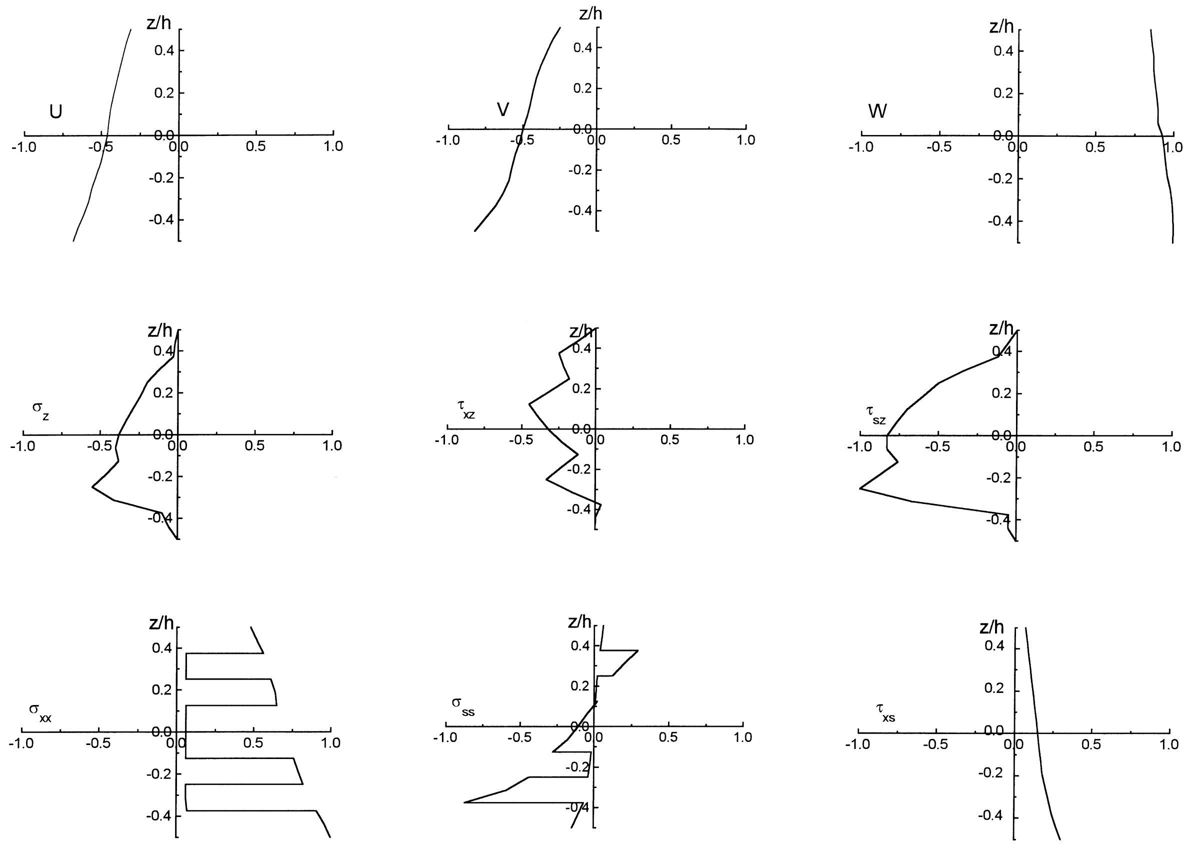

Fig. 6. Displacement and stress distributions for $n = 2$.

For $n = 2$, Fig. 6 shows significant circumferential displacement, longitudinal bending and tension. Comparing with Fig. 5, τ_{sz} gives maximum transverse stress in this case. It is also interesting to notice that the transverse normal stress becomes quite significant and may not be ignored in edge-effects analysis. The mode is associated with the end loading characterised by axial tension, bending and torsion (see the distribution of σ_{ss} and τ_{sz} and τ_{xs}).

4. Concluding remarks

The decay rates of multi-laminated hollow cylinders composed of either symmetric or antisymmetric cross-ply layers have been studied under the consideration of three-dimensional elasticity. The method is effective and can provide accurate decay rates as eigenvalues of a 3×3 matrix. The associated eigenvectors, i.e., the normalised displacement and stress distributions across the thickness of the cylinders, can also be found to show the corresponding load patterns applied at the end of the cylinders. The eigenvectors can be further used as the bases on which any self-equilibrated end loads may be expanded.

Apart from the special case concerning isotropic cylinders, the decay rates of certain moderately thick and thick cylinders with cross-ply lay-ups have been found and presented. For antisymmetric cylinders, parametric study has been performed in terms of material properties and laminate profile. It has been observed that the decay rates for laminated cylinders are in general lower than corresponding isotropic ones and the rates decrease as the cylinders become more anisotropic. It has been observed that in some cases, the characteristic decay length of anisotropic cylinders may be several times longer than the corresponding length of isotropic ones. In the cases studied in the paper, the decay rates are in general decrease as the ply number of an antisymmetric cross-ply laminate increases. However, for cross-ply laminates having more than four layers, the increase of ply number has negligible effect on the decay rates.

Along with the decay rates, the associated displacement and stress distributions were also found for some problems. From the results presented for some selected decay modes, it has been observed that any of the interlaminar stresses, including transverse normal stress, could become quite significant and therefore the edge effect of these stresses may not be simply ignored.

Appendix. Calculation of B(Z) when G has coincident eigenvalues

The Cayley–Hamilton theorem states that every square matrix satisfies its characteristic equation. As a result of the theorem, the exponential function of **G** can be represented as

$$\mathbf{B}(z) = \exp(\mathbf{G}z) = \sum_{i=0}^{n-1} \alpha_i(z)\mathbf{G}^i. \tag{A.1}$$

If λ_1 is a r-times repeated eigenvalue of **G** and the rest $n-r$ eigenvalues, $\lambda_{r+1}, \lambda_{r+2}, \ldots, \lambda_n$, are distinctive, the $\alpha_i(z)$ in Eq. (A.1) can be solved from the following linear algebra equation system:

$$\begin{aligned}
&\alpha_0(z) + \alpha_1(z)\lambda_1 + \alpha_2(z)\lambda_1^2 + \cdots + \alpha_{n-1}(z)\lambda_1^{n-1} = \mathrm{e}^{\lambda_1 z},\\
&\frac{\mathrm{d}}{\mathrm{d}\lambda_1}[\alpha_0(z) + \alpha_1(z)\lambda_1 + \alpha_2(z)\lambda_1^2 + \cdots + \alpha_{n-1}(z)\lambda_1^{n-1}] = \frac{\mathrm{d}}{\mathrm{d}\lambda_1}\mathrm{e}^{\lambda_1 z},\\
&\frac{\mathrm{d}}{\mathrm{d}\lambda_1^2}[\alpha_0(z) + \alpha_1(z)\lambda_1 + \alpha_2(z)\lambda_1^2 + \cdots + \alpha_{n-1}(z)\lambda_1^{n-1}] = \frac{\mathrm{d}}{\mathrm{d}\lambda_1^2}\mathrm{e}^{\lambda_1 z},\\
&\cdots\cdots\cdots\cdots\cdots\cdots\cdots\cdots\cdots\cdots\cdots\cdots\cdots\cdots\cdots\cdots\cdots\cdots\cdots\cdots\cdots\cdots\cdots\\
&\frac{\mathrm{d}}{\mathrm{d}\lambda_1^{r-1}}[\alpha_0(z) + \alpha_1(z)\lambda_1 + \alpha_2(z)\lambda_1^2 + \cdots + \alpha_{n-1}(z)\lambda_1^{n-1}] = \frac{\mathrm{d}}{\mathrm{d}\lambda_1^{r-1}}\mathrm{e}^{\lambda_1 z},\\
&\alpha_0(z) + \alpha_1(z)\lambda_{r+1} + \alpha_2(z)\lambda_{r+1}^2 + \cdots + \alpha_{n-1}(z)\lambda_{r+1}^{n-1} = \mathrm{e}^{\lambda_{r+1} z},\\
&\alpha_0(z) + \alpha_1(z)\lambda_{r+2} + \alpha_2(z)\lambda_{r+2}^2 + \cdots + \alpha_{n-1}(z)\lambda_{r+2}^{n-1} = \mathrm{e}^{\lambda_{r+2} z},\\
&\cdots\cdots\cdots\cdots\cdots\cdots\cdots\cdots\cdots\cdots\cdots\cdots\cdots\cdots\cdots\cdots\cdots\cdots\cdots\cdots\cdots\cdots\cdots\\
&\alpha_0(z) + \alpha_1(z)\lambda_n + \alpha_2(z)\lambda_n^2 + \cdots + \alpha_{n-1}(z)\lambda_n^{n-1} = \mathrm{e}^{\lambda_n z}.
\end{aligned} \tag{A.2}$$

References

[1] Horgan CO, Knowles JK. Recent developments concerning Saint-Venant's principal. In: Hutchinson JW, editor, Advances in applied mechanics, vol. 23. New York Academic Press, 1983. p. 179–269.

[2] Horgan CO. Recent developments concerning Saint-Venant's principle: an update. Applied Mechanics Review 1989;42:295–303.
[3] Toupin RA. Saint-Venant's principle. Archive for Rational Mechanics and Analysis 1965;18:83–96.
[4] Knowles JK. On Saint-Venant's principal in the two dimensional linear theory of elasticity. Archive for Rational Mechanics and Analysis 1966;21:1–22.
[5] Klemm JL, Little RW. The semi-infinite elastic cylinder under self-equilibrated end loading. SIAM Journal of Applied Mechanics 1970;19:712–29.
[6] Goetschel DB, Hu TH. Quantifcation of Saint-Venant's principle for a general prismatic member. Computers and Structures 1985;21:869–74.
[7] Stephen NG, Wang PJ. Saint Venant decay-rates — a procedure for the prism of general cross-section. Computers and Structures 1996;58:1059–66.
[8] Stephen NG, Wang MZ. Decay rates for hollow circular cylinder. Journal of Applied Mechanics, ASME 1992;59:747–53.
[9] Folkes MJ, Arridge RGC. The measurement of shear modulus in highly anisotropic materials: the validity of St. Venant's principle. Journal of Physics D: Applied Physics 1975;8:1053–64.
[10] Dong SB, Goetschel DB. Edge effects in laminated composite plates. Journal of Applied Mechanics, ASME 1982;49:129–35.
[11] Miller KL, Horgan CO. End effects for plane deformations of an elastic anisotropic semiinfinite strip. Journal of Elasticity 1995;38:261–316.
[12] Wijeyewickrema AC, Horgan CO, Dundurs J. Further analysis of end effects for plane deformations of Sandwich strips. International Journal of Solids and Structures 1996;33:4327–36.
[13] Tullini N, Savoia M, Horgan CO. End effects in multilayered orthotropic strips with imperfect bonding. Mechanics of Materials 1997;26:23–34.
[14] Ye JQ, Soldatos KP. Three-dimensional vibrations of laminated cylinders and cylindrical panels with a symmetric or an antisymmetric cross-ply lay-up. Composite Engineering 1994;4:429–44.
[15] Ye JQ, Soldatos KP. Three-dimensional buckling analysis of laminated composite hollow cylinders and cylindrical panels. International Journal of Solids and Structures 1995;32(13):1949–62.
[16] DeRusso PM, Roy RJ, Close CM. State variables for engineers. New York: Wiley, 1965.